A proposal of building new muon small wheels : the NSW project

Draft 0.00 30.06.2011

Abstract

abstract

1 Introduction [TK]

We propose to build a pair of new small wheel detector (NSW) to replace the existing ones during the second long shutdown[1] of the LHC during which the LHC will be upgraded to achieve its luminosity beyond the nominal design value and up to 2-3$\times 10^{34}$ cm^{-2}s^{-1} in the following running period. The goal of NSW is to bring a significant enhancement of the muon performance in the endcap region, in particular of the level-1 muon trigger as well as the precision muon tracking, that would not be achieved by simple and thus lower cost modifications alone such as improvement of radiation shielding, addition of new detector layers or upgrade of electronics.

The muon small wheel is a part of the ATLAS muon spectrometer located in the endcap region in front of the endcap toroidal magnet. This is the innermost station of the three muon stations of the endcap. There are two identical sets of detectors in both sides of ATLAS. The small wheel consists of 4+4 layers of monitored drift tubes (MDT) for precision tracking in the bending direction (R direction) and two layers of thin gap chambers (TGC) for azimuthal coordinates. These detectors cover the η range of $1.3 < |\eta| < 2.0$. The inner part of the small wheel is covered by four layers of cathode readout chambers (CSC) because of its high rate capability. Each CSC layers determines both bending and azimuthal coordinates. The coverage of the CSC chambers is $2.0 < |\eta| < 2.7$.

Just to check if reference works [1]. Once more to see the order is OK [2].

2 Upgrade motivations [TK]

Discussion of muon spectrometer performance at high luminosity - precision tracking and L1 trigger, and conclude that new detector and electronics are needed.

Point out serious (?) performance degradation in the small wheel region in both MDT and CSC, referring to the radiation background discussoin in Appendix. Performance of the present

[1] Currently it is foreseen in 2018.

detector should be evaluated for high lumi conditin, either using high lumi Monte Carlo or overlay of real events. CSC is 4 layers.

In the L1 discussion, emphasise the importance of maintaining low p_T threshold. There are two issues. the high rate of fake triggers in the endcap region based mainly on the study using data. Then introduce basic idea of how this can be mitigated by integrating the small wheel in the L1 trigger. As the second point of trigger, discuss the pT resolution and possible improvement using the new small wheel. Physics requirement asks low pT threshold (20-40 GeV), L1 rate should be maintained at 100 kHz. Need sharpening pT threshold. Here introduce 1 mrad requirement.

Finally conclude that NSW should be built and replace the present ones as a phase-1 upgrade item in preparation to running with luminosity beyond the nominal luminosity.

3 Requrements for the new small wheel [LP]

A short section with short subsections, summarising lists of requirements in numbers.

3.1 Tracking

Segment reconstruction with required performance. Resolution, efficiency, fake, ...

3.2 L1 trigger

Real-time segment reconstruction with required performance. Resolution, efficiency, fakes, ... Delay of signal availability.

3.3 Detector ageing

Integrated dose, Detector (and electronics) has to survive, or foresee replacement.

4 General Detector ..... [JD]

There are n proposed detector concepts which are discussed in next sections. Here, the following 3 points can be discussed commonly.

4.1 Mechanical structure

8+8 large-small layout, total space in z and R. Support structure, accessibility, ..

4.2 Radiation shielding

The same as now, or possible improvement of radiation shielding, ..

4.3 Alignment

Requirements, target figures, important comments which can be made independent of the detail of detector layout.

4.4 Readout electronics

Issues common to all concept. Around ROD.

4.5 DCS, services,

5 Detector concept 1 : MDT + TGC (working title)

Introduction to this concept.

This section should describe the technology concept, details up to the level of a single chamber should be given in the appropriate appendix.

5.1 Detector technology and layout

1. *Description of detector concept (a detailed description of the working principle of each detector should be given as an appendix).*
   If more than 1 technology is used motivate the decision and detail how they work together (e.g. can services be shared, is the information of the trigger chambers used in the precision chambers, how are combined chambers assembled etc.)

2. *List of all operating parameters*

3. *Detailed layout: acceptance, description of chamber overlap and dead areas, drawings*

Micromega/TGC/RPC/MDT	Type 1	Type 2
Number of chambers		
Radial extension (mm)		
Minimum length in ϕ (mm)		
Maximum length in ϕ (mm)		
Thickness in z (mm)		
Mass (kg)		
Number of layers		
Number of channels		

Table 1: Example table chamber types

Chamber	Small sector	Large sector

Table 2: Example table: Number and types of chambers per sector

4. *Tables with chambers sizes, number of channels*
5. *Internal alignment scheme (the overall common endcap alignment scheme is described in the previous chapter)*
6. *Calculations about mechanical stability and expected deformations due to gravity, temperature changes, (magnetic field) etc.*
7. *Requirements for mount points*
8. *Details of service points and other positions where access is needed*
9. *Concept for chamber replacement (what needs to be dismounted etc.)*

5.2 Performance

Summary of chamber performance, details in appendix of technology.

1. *Spatial and angular resolution as functions of rate and angle of incidence*
2. *Time resolution*
3. *Efficiency (single measurement and segment)*
4. *Double track resolution*
5. *Rejection of fake and background tracks*

5.3 L1 trigger and electronics

1. *How the L1 signal are produced, starting from the detector signal till the formation of SL input.*
2. *Latency (calculation, measurement with demonstrator)*
3. *Compatibility with Phase II upgrade*

5.4 Readout electronics and integration in DAQ

1. *Detailed description of electronics chain*
2. *Integration to DAQ*
3. *Readout related parameters, e.g. bandwidth requirements, number and granularity of read-out links*
4. *Compatibility with Phase II upgrade*

5.5 Services, infrastructure, and DCS

1. *Description of service scheme (including power system, read-out, trigger, alignment), cooling needs and other special requirements*
2. *Table with number of services (number of cables, outer diameter, cross section of leads)*
3. *Table with power consumption (per channel, chamber, total)*
4. *Required rack space*
   (a) *UX15 (include maximum allowed distance to detector if any)*
   (b) *US15 (power system)*
   (c) *USA15 (DAQ)*
5. *Gas system and distribution*
   Details on number of gas manifolds per sector (include drawings) and connections to chambers (serial, parallel?)). Size of pipes
   Required nominal, minimum, and maximum flow
   Required precision of gas mixture
   Safety measures in case of inflammable gas
   Required rack space for gas system in SGX1, USA15, UX15
6. *Integration in DCS system, requirements for DCS*

Cable	Number of cables (granularity)	Outer cable diam. (mm)	Cross section of leads (mm^2))
HV			
LV			
Monitoring and control			
Front-end links			
Calibration			
Alignment			
Miscellaneous			

Table 3: Example table number of services per chamber

Chamber	Number of channels	Power consumption per channel	Total power consumption

Table 4: Example table: Number and types of chambers per sector

6 Detector concept 2 : MDT + RPC (working title)

We propose here a dedicated trigger detector based on enhanced version of the avalanche RPCs to complement a precision tracking small tube MDT (sMDT) system in view of the SW upgrade. The choice of the RPCs as trigger detector is motivated by the extreme simplicity and robustness of this detector and even more by its excellent timing capability that, as it will be shown in this report, is crucial to reject low energy uncorrelated background in an hostile working environment. On the other hand the idea to combine a precision tracking detector with a dedicated trigger detector extends to the SW upgrade a concept that has been successfully applied to the whole muon system of ATLAS. The relatively cheap construction, the possibility of being tailored to any shape and the small amount of space it occupies, and recent breakthrough in the RPC front end allowing a great increase of the rate capability, makes the RPC detector attractive for the ATLAS SW upgrade. Moreover a substantial improvement with respect to the present muon system will be a full MDT-RPC integration concerning the mechanical structure, the electric services and the DAQ that will be based on similar ADC and TDC circuits as developed in the present MDT mezzanine cards.

Listo of partecipating Institutes The Institutes which so far have espressed interest for this project and are participating to the preparation of the present document are:

- Argonne National Laboratory
- Istituto Nazionale Fisica Nucleare Sez. Bologna (to be confirmed)
- Boston University (possible participation)
- University of Michigan
- University of Science and Technology of China
- Academia Sinica, Taiwan
- University of Roma and INFN Tor Vergata

- University of Washington

6.1 Detector technology and layout

1. **Description of detector concept** Figure 1 shows the layout of the SW detector with sMDTs as precision tracking chambers and RPCs as trigger chambers. The difference between the two angles measured by the new small wheel detector and the current EM TGCs will be used to determine the muon momentum at L1. The RPC (or mRPC as will be specified later) will be assembled together with a sMDT of equal dimensions in a common mechanical support structure which guarantees the relative alignment of the RPC to the rest muon sub-detectors in the endcap region. In order to reach the designed momentum resolution at L1, the angular resolution provided by the new small wheel detector should be about 1 mrad.

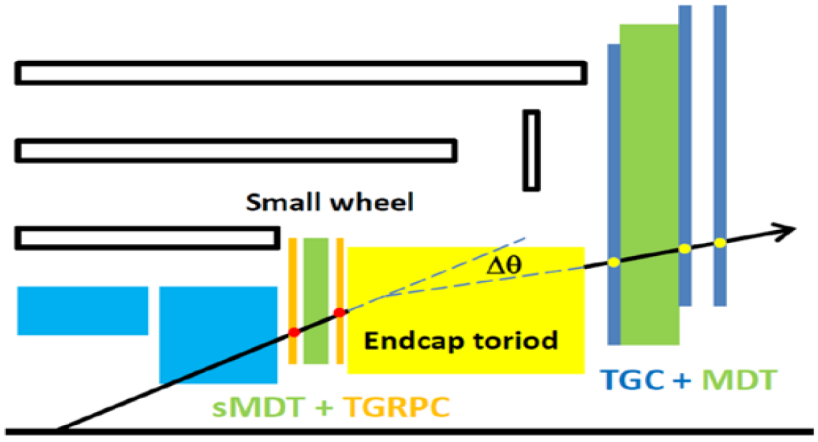

Figure 1: Detector layout for the small wheel upgrade using sMDT as the precision tracking chamber and thin gap RPC as the trigger chamber.

In order to fulfill the requirements defined for the SW upgrade, a substantial improvement with respect to the RPCs presently operating in ATLAS is needed concerning the rate capability, time resolution, position resolution and detector ageing. The ATLAS RPCs were successfully tested at a rate of 1 kHz/cm^2 and were qualified, following the ATLAS requirements, for ageing effects equivalent to 10 years operation at a rate of 100 Hz/cm^2, corresponding to 0.3 C/cm^2 integrated charge. Although larger values are acceptable for the integrated charge, we stress here that the best way to increase the RPC rate capability is to reduce the charge delivered per detected avalanche, rather than to increase the operating current using very low resistivity electrode plates [ref]. Operation at low current is indeed crucial to decrease the detector ageing and the power dissipation. For this purpose two parameters have to be optimized: the gas gap width which determines the amount of delivered charge per avalanche and the sensitivity of front end electronics which determines the minimum charge that can be discriminated from the noise.

Fast detectors are crucial to reject low energy uncorrelated background. At rates as high as 10 kHz/cm^2, a very short time (about 2 ns) coincidence between contiguous detectors is an extremely efficient method to eliminate uncorrelated hits. This requires to improve

the time resolution to $0.3 - 0.5$ ns. A thinner gap RPC would fulfill at the same time both requirements: to reduce the delivered charge and to improve the time resolution. We propose here to split the standard 2 mm gas gap of the ATLAS RPCs in two gaps of about 1 mm.

The charge centroid method applied to the RPCs allows to obtain a space resolution of the order of 0.1 mm on both coordinates. However the time required by the DAQ and the centroid computation would be too long for a 1st level trigger. We propose therefore to use narrow strips, with typical pitch of about 2 mm, coupled to a maximum selector circuit that should give the centroid position within 0.3 mm.

The RPC is a gaseous parallel electrode-plate detector whose working principle has been already described in detail [ref]. The Atlas RPCs presently working in the barrel are based on a 2 mm gas gap between two resistive electrodes 2 mm thick, made of a melamine coated phenolic laminate that is usually (and improperly) referred to as bakelite. The gas volume just described is sandwiched between two read out panels with mutually orthogonal strips giving a point in the space for each avalanche generated inside the gas. The low p_T stations are made of two RPC doublets, with the MDTs in the middle, and giving 4 points along the muon track with a trigger logics requiring a 3 out of 4 coincidence.

The scheme we propose for the SW upgrade is conceptually very similar to that just described, with the following differences required by the more difficult working conditions with respect to the barrel.

- The single 2 mm gas gap is split into two 1 mm gaps giving the advantages of a better time resolution, a lower delivered charge which increases the rate capability and a higher efficiency due to two gaps inducing simultaneous signals on the same strips. We will refer to this type of RPC as mRPC for its double (multiple) gap.
- The electrode thickness is reduced to 1 mm not to increase the average distance of the avalanches generated in the gas from the pick up strips in a two gaps structure.
- The two doublets structure is improved to two triplets (Fig. 2). This allows to make very short time coincidences among detector layers of the same triplet, thus strongly reducing the uncorrelated background. The trigger logics requires the 2 out of 3 coincidence inside the same triplet followed by the twofold coincidence of the two triplets signals.
- The eta strips width is strongly reduced to improve the angular resolution in the bending view. Typically a 2 mm strip pitch is foreseen. The thin strips are grouped in super-strips 12 mm wide connected to a maximum selector which identifies, in a typical time of 10 ns, the mini-strip of maximum charge, which gives the best position for the track.
- The strips of at least one of the two views will be equipped with both ends read out connected to a mean-timer circuit. This will improve the trigger performance for two fundamental reasons:
  (a) The track position will be localized along the strip with a typical uncertainty of a few cm giving a further reduction of uncorrelated background in the coincidence of two contiguous chambers;

(b) In case of two or more muons crossing the same chamber the simultaneous measurement of both coordinates on the same strip will remove ambiguities and ghost hits.

- A further fundamental concept of this proposal is the idea to substantially increase the front-end electronics sensitivity and signal to noise ratio, and to reduce consequently the required gas gain amplification. The low gas gain operation is indeed of crucial importance to increase the rate capability without increasing at the same time the power dissipated inside the gas and the ageing of the detector. Test of RPCs equipped with a new front-end circuit [ref] have shown that a factor of at least 7 in terms of total charge delivered in the gas, and thus in rate capability, can be achieved.

Our baseline proposal is based on a triplet of 1+1 mm bi-gap mRPCs. Figure 3 shows two possible configuration of the bi-gap being considered, the topmost is the classic mRPC configuration with a floating central electrode; below is shown a bi-gap made essentially of two electrically independent single gap detectors being read externally by the same readout strip planes. However the overall project is aimed to optimize rate capability, background rejection, mechanical robustness and number of read out channels. This many parameter optimization requires accurate simulations that are not yet been made. We are therefore keeping on study other possible configurations.

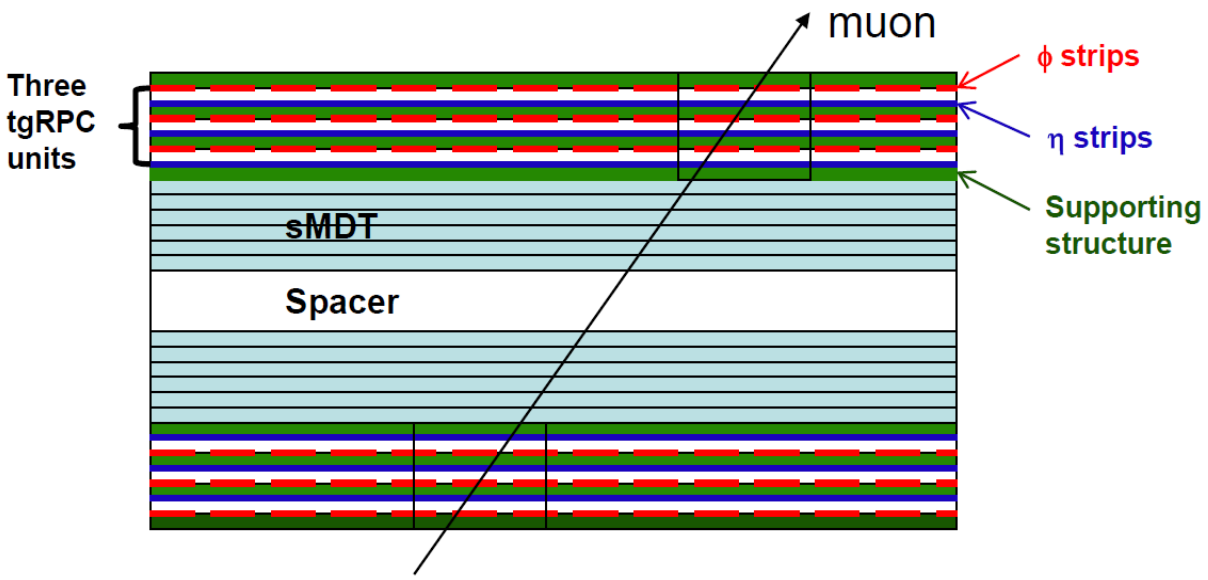

Figure 2: Layout of the mRPC detector with three units on both sides of the sMDT chamber. Each mRPC unit will be read out along both eta and phi directions.

2. **List of all operating parameters**

Table 5 summarize the present baseline chamber parameters. Further parameter fine tuning is under study so this numbers are suitable to change. The detector structure inherits most features (except thickness) from ATLAS experience. Readout strips along eta and phi directions are placed on the outer surface of the bakelite electrode plates. All plates have a thickness of 1 mm and a volume resistivity of $\sim 10^{10}$ Ω cm. The gas gap size is 1mm, and the correct distance between two plates being assured by a grid of spacers.

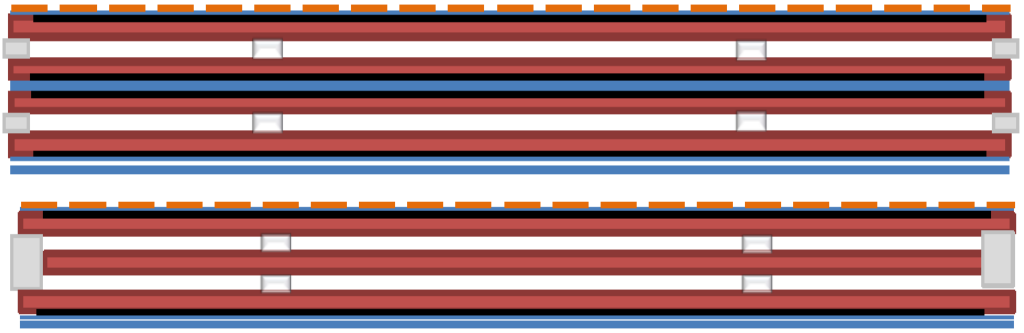

Figure 3: Two possible configurations for each mRPC detector. Top: classic multi-gap configuration with the inner floating electrode; Bottom: a bi-gap made of independent single gap detectors. Each mRPC will be read out along both eta and phi directions.

Parameter	Design value
Operation mode	Avalanche
Timing resolution	<0.5 ns
Rate capability	10 kHz/cm^2
Gas gap	1 mm
Bakelite plate thickness	1 mm
Bakelite resistivity	$\sim 10^{10}\Omega$ cm
Prompt Eta-hit position resolution	0.3 mm
Prompt Phi-hit position resolution	3 mm
Off line Phi-hit position resolution	0.3 mm
Eta-strip pitch size	2 mm
Phi-strip pitch size	0.8 - 2 cm
Gas mixture	$C_2H_2F_4$/ Iso-C_4H_{10}/SF_6 (94.7/5.0/0.3)
Operating voltage	$\sim$ 6 kV (12 kV for the floating electrode bi-gap version)

Table 5: Parameters for the mRPCs. All the values are still to be considered as approximate

Graphite layers with surface resistivity of 100 kΩ, transparent to the fast RPC signal, are painted on the external surfaces of resistive plates, to distribute the high voltage. A 100 μm insulating foil of PET separates the graphite electrodes from the readout.

The high voltage to be applied to each gas gap is $\sim$ 6 kV allowing the RPC running with a low gain avalanche mode enhancing the detector rate capability. The gas mixture of C2H2F4/Iso-C4H10/SF6 (94.7/5/0.3) used by the current ATLAS barrel RPCs is also expected to be used for the proposed mRPC detector.

The detector layers are interleaved with two support panels made of light-weight paper honeycomb and are held in position by a solid frame of aluminium profiles. The total thickness of a mRPC unit with bakelite plates and gas gap readout PCB board is about 10 mm thus the triplet can easily fit the tight space budget for the SW upgrade, including some support structure. Further optimization is under study for the integration of the RPC and MDT chambers in a hybrid single piece of detector.

The main operating parameters for the proposed mRPC detector are given in Table 5.

3. **Detailed layout: acceptance, description of chamber overlap and dead areas, drawings**

The layout of the mRPC detector will follow the layout of the sMDT system with large and small sectors. The layout of the large and small sectors of the new small wheel can be found in Fig. 6. The mRPCs we propose will cover the pseudorapidity range of $1.05 < |\eta| < 2.7$ and be mounted on both sides of the sMDT chambers with readout strip position referenced to the sMDT tubes for internal alignment. The azimuthal angle coverage is 100% due to the overlap of the small and large sectors.

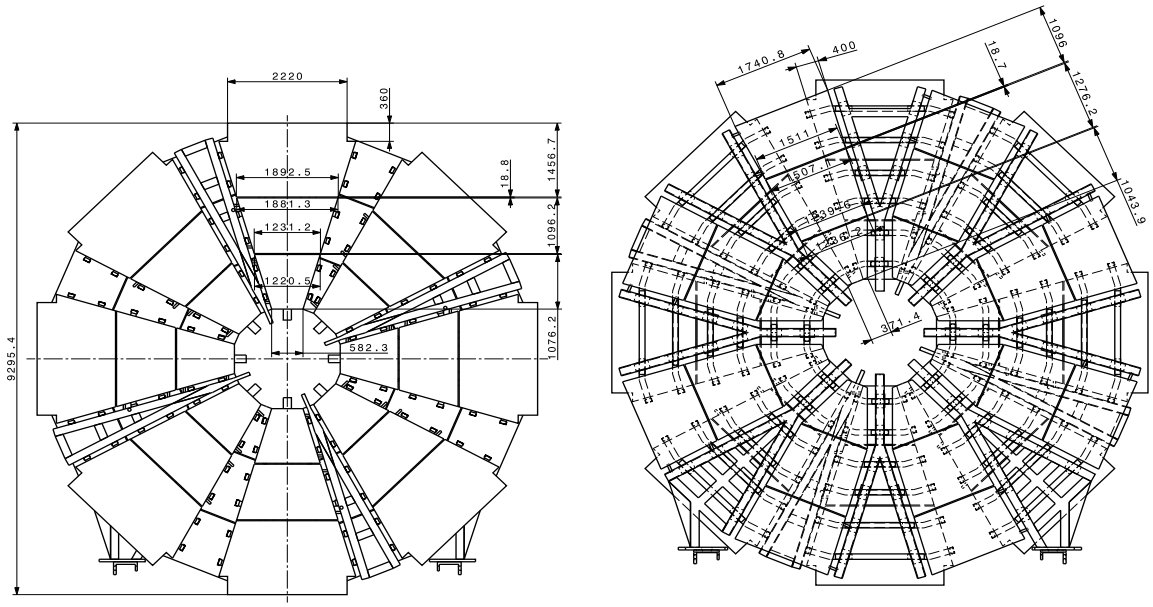

Figure 4: Layout of large (left) and small (right) sectors.

4. **Tables with chambers sizes, number of channels**

   In total, there will be six types of mRPC chambers with different sizes, three for big sectors and three for small sectors. There will be 48 chambers in total for each wheel. All chambers have a trapezoidal geometry, and the covered area ranges from 0.9 m × 1.1 m to 2.0 m × 1.5 m for large sectors and from 0.8 m × 1.0 m to 1.6 m × 1.1 m for small sectors. Details can be found in Table 7 and 6.

   With an eta-strip readout pitch of 2 mm and readout from both ends, the total number of readout channels is estimated to be 225.4 k for both wheels. The total number of readout channels is calculated using the sum of readout channels in Table 2 multiplied by 8 for eight sectors (both large and small sectors) and 2 for wheels on A and C sides.

5. **Internal alignment scheme (the overall common endcap alignment scheme is described in the previous chapter)**

   A mRPC will be glued on the surface of a sMDT chamber with similar dimensions. The relative position of the mRPC to the sMDT is expected to be within 50 microns. The internal alignment of the RPC depends on the precision of the readout strips on the PCB. A strip position precision of 25 microns (???) for readout strips on a PCB is expected.

Chamber type	η channels per chamber	ϕ channels per chamber	Total channels per wheel	Total Power per wheel (W)
Big sector, type I	3240	1500	37920	758
Big sector, type II	3240	1500	37920	758
Big sector, type III	4320	1500	46560	931
Small sector, type I	3240	1200	35520	710
Small sector, type II	3960	1200	41280	826
Small sector, type III	3240	1200	35520	710
Total per wheel	21240	8100	234720	4694

Table 6: Channels and power statistics for six types of mRPC chambers and for the whole New Small Wheel.

Chamber type	Chamber geometry (top/bottom/height) (mm)	Num of layers $\times$ chambers	Phi pitch (mm)
EIL0	2400/1892.5/1456.7	3×2	20
EIL1	1881.3/1231.2/1096.2	3×2	14
EIL2	1220.5/582.3/11076.2	3×2	8
EIS0	1740.8/1511.0/1096	3×2	20
EIS1	1507.1/1239.6/1276.2	3×2	14
EIS2	1236.2/371.4/1043.9	3×2	8

Table 7: Detector dimensions for six types of tgRPC chambers and the corresponding number of readout channels per sMDT-tgRPC unit. The factor of 4 counts for readout from both ends and two doublets on a sMDT chamber.

6. **Calculations about mechanical stability and expected deformations due to gravity, temperature changes, (magnetic field) etc.**

   Since the mRPC will be directly integrated on the surface of a sMDT, the flatness and the mechanical stability should be similar as the sMDT chambers. The mRPCs have small size and will be installed vertically, the gravity effect will be negligible. The temperature and magnetic field effects should be small and will be monitored by the MDT temperature and magnetic field monitoring system.

7. **Requirements for mount points**

   The mount points are on sMDT chambers and no mount points are needed for mRPC.

8. **Details of service points and other positions where access is needed**

   Each sector will have one gas inlet and one gas outlet with fanout/fanin to each chamber. High voltage for each sector will be applied through high voltage splitting boxes similar as used for the current MDT system.

9. **Concept for chamber replacement (what needs to be dismounted etc.)**

   The whole sMDT-mRPC unit needs to be dismounted if we need to replace either the sMDT or the mRPC.

6.2 Performance

In this section firstly is described the performance and features of the single RPC detector element. Basing on this the features of the proposed RPC based subsystem will be analyzed.

6.2.1 The single gap RPC intrinsic performance

The RPC sensitive volume is a thin layer of gas confined between parallel resistive electrodes, establishing an uniform field in it and allowing a prompt signal production. The fast electron avalanche signal can be read by means of external electrodes on which a 2D charge distribution is induced by the growing avalanche.

The 2D charge distribution has and approximative gaussian shape whose width is essentially dependent on the gas gap and electrodes thickness [**?**] [**?**]. For instance for an ATLAS standard RPC (2 mm gas gap and 2 mm electrodes thickness) the FWHM of the charge distribution is about 6 mm as shown in fig.**??**. An enhanced layout of 1 mm gas gap and 1 mm thick electrodes will produce a charge distribution with halved width. The impact point of the particle is localized on the transversal plane though the position the charge distribution maximum, within a few hundreds of microns in each direction, depending on the detector layout. In a recent test a resolution of $\sim 300\ \mu m$ has been measured at the H8 test beam with a non optimal 13 mm pitch strip readout panel **??**, using the charge centroid method.

Has been shown that the 2 mm gas gap have a time resolution of $\sim$ 1 ns and has been demonstrated that this enhances inversely with the gap width [**?**, **?**]. In figure **??** the signal development for different gap width is compared. For 1 mm gas gaps a time resolution of about 0.5 ns is expected

The gas gap intrinsic efficiency, thus the ability of producing a detectable avalanche, depends essentially on the primary ionization statistics of the incident particle on the gaseous target. The ionization density of a MIP for the ATLAS gas mixture is about 15 couples/mm. Being the first fraction of the available gas target suitable for an efficient avalanche detection, the inefficiency is still negligible for 1 or 2 mm gas gaps while some efficiency loss is visible for a 0.5 mm gas gap as clearly visible in fig. **??**. A fixed inefficiency contribution of about 1% has to be considered due to spacers and frames. The gas gain depends on the applied field and its fluctuations are dominated by the initial position of the very firsts electron/ion couples. Due to the space charge saturation effects the charge tend to grow linearly with the drift space [**?**], producing a compression in the charge distribution dynamics and a peaked shape.

The avalanche detection has to do with the signal to noise ratio of the ensemble constituted by the RPC and its readout system, thus it cannot be disentangled from the front end amplifier design and performance: The higher is the performance of the last the lower is the gain requested in the gas for a given efficiency. This has an obvious consequence on the detector rate capability and ageing performance. A newly developed frontend amplifier applied to an ATLAS like RPC permitted a substantially lower working point corresponding to a factor of 10 less charge delivered per count. A test performed at the CERN GIF with this frontend demonstrated a full efficiency detection for triggered cosmic rays while counting 8 KHz/cm^2 of photons illuminating the whole chamber surface (fig. **??**).

The response of an RPC to large ionization events is determined by two facts: The saturated avalanche operating mode and the resistive electrodes. The saturated avalanche growth, as described in [**?**], is linear with increase of drift space or electric field until the limit for generating a streamer is reached. Similarly a fluctuations of the primary ionization has a slight effect on the total charge. This mechanism is making extremely unlikely the generation of a streamer but even in this extremal case the streamer charge is only about a factor of 10 larger than the avalanche and anyhow the bulk resistive electrodes have the fundamental property of self extinguishing the charge multiplication [**?**] due to a local field depletion which is restored slowly with respect to the discharge time constant.

6.2.2 The overall performance of the SW RPC stations

Hereby follows the analysis of the proposed RPC station performance as tracking trigger. The baseline design consists in two RPC chambers sandwiching the sMDT chamber, each chamber being a triplet of 1+1 mm bi-gaps as shown in fig. **??** and described in 6.1. Each gap is readout by orthogonal strip planes. The strip pitch is $\sim$ 1-2 cm in the ϕ coordinate while the bending coordinate η is segmented in strips of 2 mm pitch. All the strips are equipped locally with a newly developed extremely sensitive front end amplifier allowing the RPC signal detection with a factor of 10 less charge delivered in the gas with respect to the present ATLAS RPCs. The full features of this circuit will be described in Section 6.4.

The ϕ strips are readout by means of the same readout cards used for the sMDTs providing 0.3 ns timing and charge readout. The Eta strips are read in groups of 8 (a super-strip) by an especially developed circuit, the Maximum Selector (MS since now), allowing to extract from the charge distribution the strip or the strips having the maximum induced charge. A fast mean-timer circuit (MT since now) has also been developed with a resolution of 250 ps. It will process the signal coming from both ends of a η super-strip allowing to promptly locate the particle impact event in a very narrow space-time region of $\Delta\eta \times \Delta\phi \times \Delta t = 1cm \times 5cm \times 2ns$. Both circuits will be described in Section 6.4. Optionally a solution having the MT placed on the ϕ strips to minimize the channel number is being studied.

The different features performance list:

1. **Spatial and angular resolution as functions of rate and angle of incidence**. The space resolution for orthogonally incident MIPs on a single detector plane:

   - for *phi* strips $\sim$ 1 cm $/\sqrt{12}$ (promptly) and $\sim$ 0.3 mm with off-line calculation the charge centroid
   - for $\eta \sim$ 0.3 mm by means of the maximum selector. This is calculated as follows: $0.5 \cdot strip\_pitch/\sqrt{12}$, where the factor 0.5 is coming from the exploiting of the cluster size 1 and 2

   Given the lever arm of about 40 cm this would already satisfy the angular resolution < 1 mrad. The presence of at least 2 points per RPC chamber further enhances the angular resolution. The final result depends on strip alignment details of the chamber layout which are not yet fixed.

2. **Time resolution** A single 1 mm gas gap has a resolution of about 0.5 ns, which further improves in the 1+1 mm bi-gap configuration since the timing goes with the OR of the two sub-gaps. An exact estimation will be calculated and tested. Further timing enhancement, valuable for TOF applications is provided by the multiple measurements done by the two triplet chambers

3. **Efficiency (single measurement and segment)** With 1 mm gaseous target thickness an efficiency of about 99% can be achieved by the single gas gap. Nonetheless this is not the best in terms of charge per count economy. The multi-gap structure with common readout in facts allow to:

   - achieve high efficiency
   - limit the charge per count
   - minimize the number of channels
   - improve the timing

   The first two points are determined by the fact that the most of total charge per count delivered is due the the last 10% of efficiency, due to the avalanche growth dynamics. Therefore a big advantage is coming from subdividing the gap in sub-gaps in OR with respect to the delivered signal. Moreover the total delivered charge for a given signal amplitude is 1/N where N is the number of sub-gaps [**?**]. For example operating the single sub-gaps of a bi-gap at 90% of efficiency would result in efficiency ¿99% with a factor of ~ 4 of saved charge per count, by combining the two effects.

   A similar logic suggest to implement a 2/3 majority coincidence in each chamber to individuate the muon segments. Each segment is individuated by at least 2 points per chamber. To make an example the failure probability of the single chamber is less than 0.5% for single bi-gap efficiency of 96% (corresponding to a sub-gap efficiency of 80%); the segment failure probability given by the AND of the two chambers is less tan 1%.

4. Double track resolution The double track resolution for the trigger is driven by the maximum selector granularity in η and the strip pitch in ϕ, both of the order of 1-2 cm. The mean-timer readout using the information from both end of one of the strip planes permit to eliminate the ghosts: two real hits on the same detector, read by strip planes on the two coordinates, would give rise to 4 potential hit points at the crossing of each couple of strips. The mean timer eliminates the ambiguity is the hits are more than 5 cm distant in the mean timer coordinate.

5. **Rejection of fake and background tracks** The high level of background is a potential source of fake triggers. This can come by random coincidences of photon hits, largely dominating the background or by a combination of this and low energy charged tracks, which are mostly synchronized with the real tracks and able to trigger at least one of the two chambers. The RPC detector design will exploit the space-time detector performance to minimize this fake contribution. Here follows a simple calculation of fake rate based on the proposed layout more details are given in section 6.3:

   - We assume 10 kHz/cm^2 and the maximum background rate

- the mean-timer applied to a single mRMC selects an area of $\sim 1.6\times5$ cm^2. Figure 5 shows the benefit of using mean-timer to determine the hit position along the phi strip.
- The RPC time resolution and the mean-timer allow a $\pm3\sigma$ time window of ~ 3 ns for the 2/3 majority. This produce a chamber fake rate on a 8 cm^2 virtual pad of:

$$(0.8 \cdot 10^5 Hz) \times (7.2 \cdot 10^5 Hz) \times 3 * 10^{-9} s * 3(times) = 518 Hz$$

- since one 1m^2 chamber contains 1250 virtual pads (320 kHz per chamber) , the final coincidence of the two chambers sandwiching the sMDT, gated at about 10 ns, produce a fake rate of:

$$(\sim 650 kHz)^2 \times 10^{-8} s \simeq 4.2 kHz$$

- This value can be further reduced by cutting in solid angle, accepting only the hit configuration corresponding to pointing tracklets. This function can be performed at the end of the trigger chain on all the proposed tracks, by means of a jump table
- Another background source arise from the low energy charged particles with an energy sufficient to trigger the first chamber. Even if small fraction of the total background is constituted by this type of events the fake rate increase substantially. For instance 1% of the background already corresponds to 1MHz/m^2 of triggers in the first chamber, which can coincide with a random hit on the second chamber. The strongest possible suppression of random hits is the best way to suppress also this type of background.

6.3 L1 trigger and electronics

(a) **How the L1 signal are produced, starting from the detector signal till the formation of SL input**

The combination of segments found by the mRPC and the EM TGCs will be very useful to reject uncorrelated backgrounds. Due to the excellent RPC time resolution every single hit can be selected on the base of a very strict space-time coincidence. The maximum selector electronic circuits that can determine the center of the clusters of fired strips is gated by this coincidence and deliver the hits to a segment trigger processor that performs the muon segment search. This segment trigger processor searches for coincidences with the predefined patterns of four strips in two doublets (equals to four single gas gaps) among the surviving hits. In particular these segments are required to roughly point to the IP not to be rejected, as shown in Fig. 7.The second coordinate coincidence is also required to reduce the amount of fake muons due to uncorrelated background hits and detector intrinsic noise. Another muon trigger processor receives the segments sent by the EM TGC trigger and combines them with the segments sent by the mRPC trigger. It performs a matching based on the proximity of the segments in the η and ϕ space. If the two segments are close, the angle difference is then used to determine the momentum of the muon passing through. If the segments are too far away from each other, the two segments will be thrown away and will not be considered to form a muon. Special attention

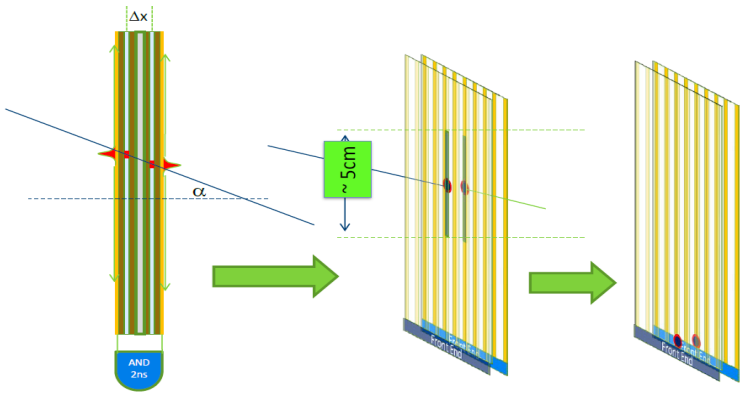

Figure 5: Benefit of using mean-timer electronics to determine the hit position along the phi strip. This will simplify the level 1 trigger algorithm and reduce random rate.

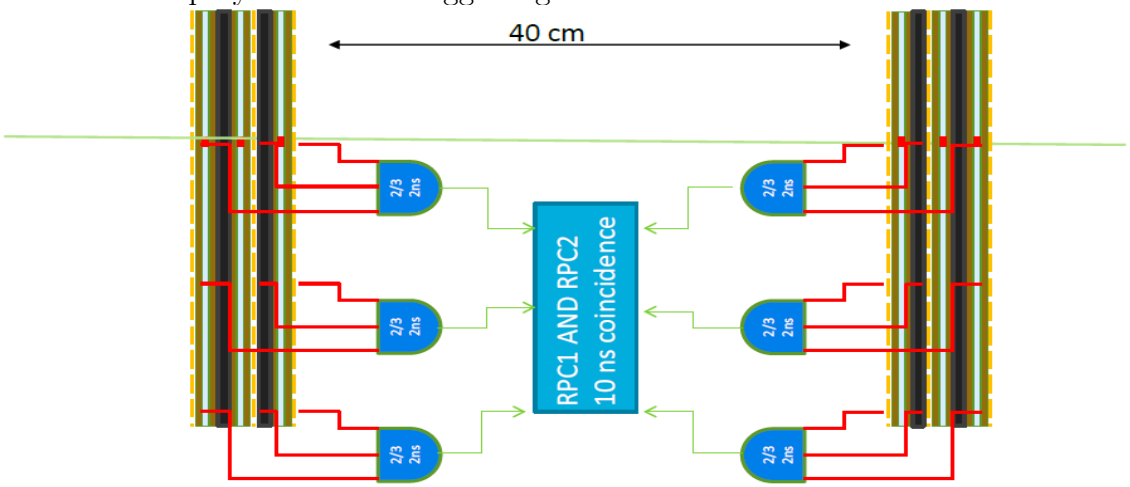

Figure 6: Layout of L1 trigger. The output from the maximum selector will be used to form the small wheel segments.

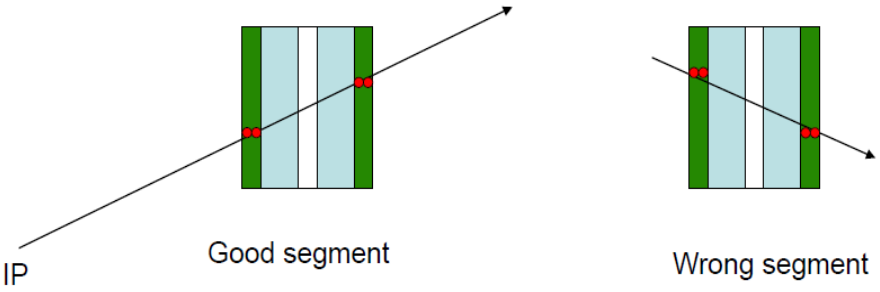

Figure 7: The segments determined by the new small wheel detector need to point to the IP. Segments that are not pointing to the IP will be rejected.

needs to be given to the overlap region to avoid the same muon reconstructed twice. All successful fitted muons are sent to MUCIPi for further processing.

The whole covered area is 35.4 m2 for small sectors and 43.7 m2 for big sectors, within a period of 25 ns, the average number of random hits expected for the whole covered area by the small wheel is about 200.

Targeting Precise Signal timing

The proposed design focuses on precise timing aided by differential measurements from both ends of the strips. A combination of these measurements provides exceptional signal timing via digital mean timers and a second coordinate is available from differential timing for background rejection purposes. The development of a second coordinate within a single layer eliminates ambiguities even at the highest rates. The precision of the second coordinate is far less than that available from the strips and is expected to be on order of a few centimeters. The second coordinate precision will be known from test on early version with the aid of off-line evaluation of the differential readout.

(b) **Compatibility with Phase II upgrade**
A small number of synchronous, 2 dimensional coincidence trigger segments from each azimuthal region would be natural to combine with the TGC trigger elements from the Big Wheel either at the existing trigger crates or at new crates located in USA-15. The results would be a confirmed high-Pt muon with a sharpened threshold.

(c) **Latency**
The signal will arrive through the amplifier-shaper-discriminators and the digital-mean-timer a few tens nanoseconds after it is generated inside the detector. This takes in to account the arrival of signals from the most distant end of the strip and the cabling delays. A further delay of about 10 ns will be added by the coincidence requirements associated with the maximum selector. Thus, after a fixed delay < 100 with respect to the crossing, a two coordinate data unit is available. How many such units are to be processed in parallel awaits detailed simulations. One could imagine that a 2 out of 3 coincidence from 3 layers might be used on-chamber to reduce backgrounds by demanding pointing toward the IP, within appropriate cuts, to select high momentum and remove off angle tracks from a crude polar cut. A SW latency value consistent with the BW TGC should be easy to accomplish. Knowledge of the rejection of spurious hits will only be understood with detailed simulations.

Evaluation of the Trigger Scheme
We will make use of the ATLAS muon monitored drift tube (MDT) front-end readout electronics for testing the proposed mRPCs and the proposed trigger scheme. This test system can accept trigger and readout signals at MHz rates for burst periods to test the high rate capability of the detector. Certain modifications and developments are needed to get the signals from both ends the mRPCs. The readout is pictured in Fig. **??**.

In figure 8 the details of the electronics equipment of the η strip panel. On the side of the maximum selector, which reads out groups of 8 strips, one amplifier per strip is used. The maximum selector provides also the average charge of the strip group which is used by the meantimer. On the other end of the strip the analog sum of the same 8 channels is also amplified and delivered to the mean-timer. The cable length is adjusted within 100 ps tolerance.

- We will use offline computation of the differential timing from both ends to determine the hit position along the strip with a resolution of 5-10 cm.
- We will examine the need for an analog peak selector-digital encoder.
- We will compute the mean time of the signals read from both ends and examine the role of fast timing in the suppression of backgrounds. We will examine the suppression of combinatorial background using timing within a layer vs.

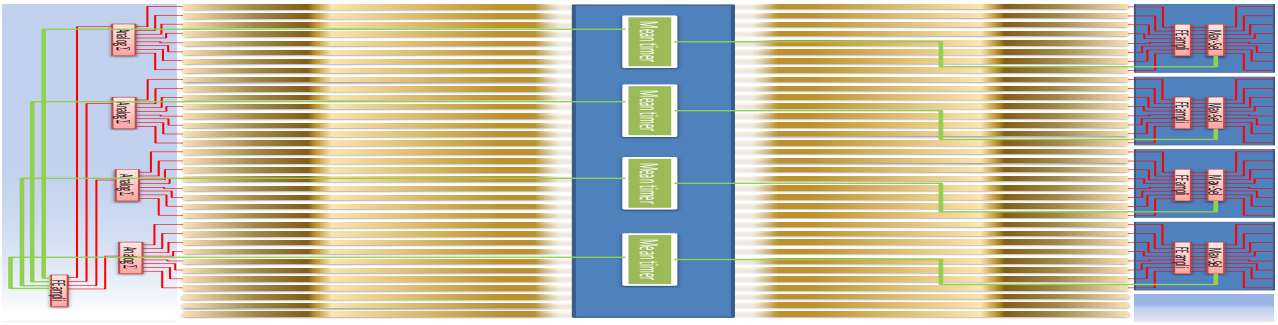

Figure 8: η strip panel readout and space-time localization electronics.

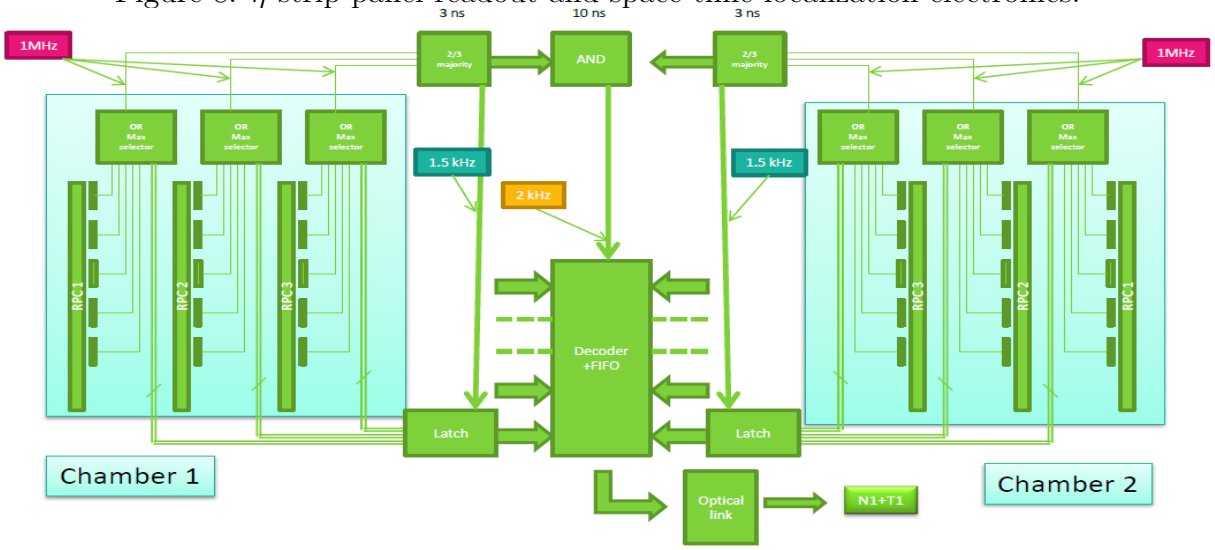

Figure 9: Layout of readout electronics.

multilayer timing.

- We will examine the precision in the bend direction to assess whether the proposed chamber can meet the ¡ 1 mr requirement with the level arms possible in the SW layout proposed.
- An optimal layout considering the number of layers, strip separation, coincidence timing, and circuit modularity will be examined.
- We will assess the background hit rejection of all algorithms considered.

6.4 Readout electronics and integration in DAQ

(a) **Detailed description of electronics chain**

The readout proposed for the data stream is to be shared with the MDT which requires a redesign of the mezzanine cards for higher density, higher serial readout rate, and repair of the pair modedifficulty. This also includes a redesign of the CSM to incorporate the GMT chip and up to date radiation hard electronics.

If the goal of on-chamber multi-layer coincidence can be met, the large channel count electronics will be limited to the chamber level. For the trigger this would be arranged as synchronous fiber output of a small number of SW segments selected to

be pointing toward the IP within a high momentum requirement in the polar angle and an appropriate match in azimuthal angle.

For the data readout, hits need be stored in rather large level-1 buffers awaiting a trigger signal. For the MDT the readout window will be programmed to accept the full drift time as is now the case. For the mRPC the readout window can be quite small so readout rates will be smaller even with the large channel counts of the mRPC. Two modes of mRPC hit storage are likely, one that saves all hits and one that retains only hits that combine to form trigger segments. In a design that must include programmed timing alignment of signals from different layers for ns level timing, the first mode is necessary to tune the time alignment. A scheme of this kind was used in CDF where a custom IC (called the data phase chip) was included to provide time alignment of signals.

With a mRPC with 1.25 mm strip repeat 2400 channels per meter signals leave both ends of the detector and converge at a front-end board where regional trigger primitives are generated. It is anticipated that a small number of selected segments will each leave this regional board on a synchronous (to the crossing) fibers. Data for readout upon a level-1 trigger will be stored on the regional board awaiting a level-1 trigger. This is similar to the current mezzanine and CSM design. Whether this mezzanine card equivalent sends its data to a shared CSM equivalent or an independent multiplexer is a design question. In either case the data format and design characteristic of the multiplexer are to be the same. Todays multi-conductor micro-coaxial cables are capable of 0.625 mm intervals.

The cable cross section to the regional board for both ends assuming 1mm packing of the 0.625 mm cables is 50 cm2/meter of detector width for all 3 layers of a 3 layer system. This appears to be quite doable. If the process of combining these signals into a small number of synchronous fibers for trigger and a small number of asynchronous fibers for readout, outgoing cable cross sections to the CSM equivalent will be small. A token passing scheme would permit the front-end cards to compact many channels into a single fiber for transmission to the multiplexer.

(b) **Integration to DAQ**

(c) **Readout related parameters, e.g. bandwidth requirements, number and granularity of read-out links**

(d) **Compatibility with Phase II upgrade**

This needs a decision of how the new MDT redesign of the mezzanines and CSM are changed. I think we should move to a token passing scheme for transmission between mezzanine cards (something the current AMT chip can do we do not use it). In such a scheme each mezzanine passes its request to send data to the next mezzanine with the last sending everyones data to a small fiber board for transmission to the CSM which can be far away if desired. Such a scheme lends itself to the mRPC which has many channels arriving at a single front-end board.

6.5 Services, infrastructure, and DCS

(a) Description of service scheme (including power system, read-out, trigger, alignment), cooling needs and other special requirements

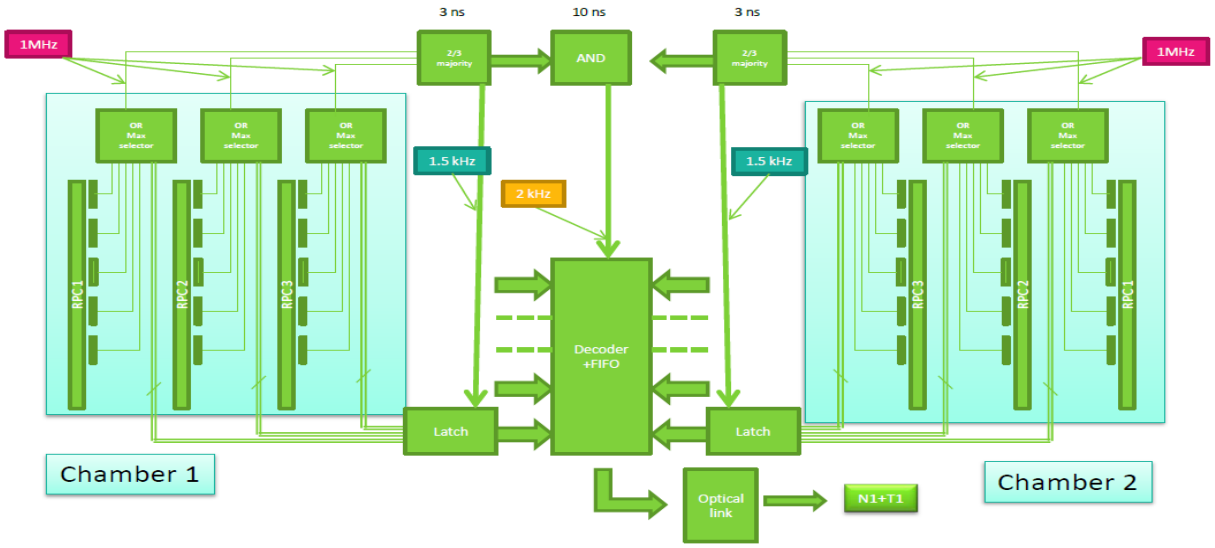

Figure 10: Layout of readout electronics.

Cable	Number of cables (granularity)	Outer cable diam. (mm)	Cross section of leads (mm^2))
HV			
LV			
Monitoring and control			
Front-end links			
Calibration			
Alignment			
Miscellaneous			

Table 8: Example table number of services per chamber

(b) *Table with number of services (number of cables, outer diameter, cross section of leads)*

(c) *Table with power consumption (per channel, chamber, total)*

(d) *Required rack space*

   i. *UX15 (include maximum allowed distance to detector if any)*

   ii. *US15 (power system)*

   iii. *USA15 (DAQ)*

(e) *Gas system and distribution*
Details on number of gas manifolds per sector (include drawings) and connections to chambers (serial, parallel?)). Size of pipes
Required nominal, minimum, and maximum flow
Required precision of gas mixture
Safety measures in case of inflammable gas
Required rack space for gas system in SGX1, USA15, UX15

(f) *Integration in DCS system, requirements for DCS*

Chamber	Number of channels	Power consumption per channel	Total power consumption

Table 9: Example table: Number and types of chambers per sector

Micromega/TGC/RPC/MDT	Type 1	Type 2
Number of chambers		
Radial extension (mm)		
Minimum length in ϕ (mm)		
Maximum length in ϕ (mm)		
Thickness in z (mm)		
Mass (kg)		
Number of layers		
Number of channels		

Table 10: Example table chamber types

7 Detector concept 3 : Micromegas (working title)

Introduction to this concept.

This section should describe the technology concept, details up to the level of a single chamber should be given in the appropriate appendix.

7.1 Detector technology and layout

(a) Description of detector concept (a detailed description of the working principle of each detector should be given as an appendix).
If more than 1 technology is used motivate the decision and detail how they work together (e.g. can services be shared, is the information of the trigger chambers used in the precision chambers, how are combined chambers assembled etc.)

(b) List of all operating parameters

(c) Detailed layout: acceptance, description of chamber overlap and dead areas, drawings

(d) Tables with chambers sizes, number of channels

(e) Internal alignment scheme (the overall common endcap alignment scheme is described in the previous chapter)

(f) Calculations about mechanical stability and expected deformations due to gravity, temperature changes, (magnetic field) etc.

(g) Requirements for mount points

(h) Details of service points and other positions where access is needed

(i) Concept for chamber replacement (what needs to be dismounted etc.)

Chamber	Small sector	Large sector

Table 11: Example table: Number and types of chambers per sector

7.2 Performance

Summary of chamber performance, details in appendix of technology.

(a) Spatial and angular resolution as functions of rate and angle of incidence

(b) Time resolution

(c) Efficiency (single measurement and segment)

(d) Double track resolution

(e) Rejection of fake and background tracks

7.3 L1 trigger and electronics

(a) How the L1 signal are produced, starting from the detector signal till the formation of SL input.

(b) Latency (calculation, measurement with demonstrator)

(c) Compatibility with Phase II upgrade

7.4 Readout electronics and integration in DAQ

(a) Detailed description of electronics chain

(b) Integration to DAQ

(c) Readout related parameters, e.g. bandwidth requirements, number and granularity of read-out links

(d) Compatibility with Phase II upgrade

7.5 Services, infrastructure, and DCS

(a) Description of service scheme (including power system, read-out, trigger, alignment), cooling needs and other special requirements

(b) Table with number of services (number of cables, outer diameter, cross section of leads)

(c) Table with power consumption (per channel, chamber, total)

(d) Required rack space

i. UX15 (include maximum allowed distance to detector if any)

ii. US15 (power system)

iii. USA15 (DAQ)

Cable	Number of cables (granularity)	Outer cable diam. (mm)	Cross section of leads (mm^2))
HV			
LV			
Monitoring and control			
Front-end links			
Calibration			
Alignment			
Miscellaneous			

Table 12: Example table number of services per chamber

Chamber	Number of channels	Power consumption per channel	Total power consumption

Table 13: Example table: Number and types of chambers per sector

(e) Gas system and distribution
Details on number of gas manifolds per sector (include drawings) and connections to chambers (serial, parallel?)). Size of pipes
Required nominal, minimum, and maximum flow
Required precision of gas mixture
Safety measures in case of inflammable gas
Required rack space for gas system in SGX1, USA15, UX15

(f) Integration in DCS system, requirements for DCS

8 Expected muon performance with NSW [SV]

Discussion of overall performance. L1 trigger, muon reconstruction, efficiency, fake, sensitivity to a few layout parameters (number of layers, ...),

9 Integration, assembly and commmissioning [JD]

10 Cost, resources and schedule [LP, TK]

11 Conclusions

Appendices

A Radiation background

Discussion of expected cavern background and its uncertainty based on simulations and measurements with muon detectors, and finally give a reference figures and safety factor.

- *Overview of cavern background. It's nature, origin, shielding strategy*
- *Simulation result. R distribution in the small wheel region. 14 TeV, Al beam pipe, 14 TeV steel beam pipe, 7 TeV steel beam pipe.*
- *Measuremenents with pp collision. MDT, CSC*
- *Summary figure. Reference figures.*

A.1 simulation

B Small tube

Detail of detector technologies proposed for use in the small wheel detector, including the status of developments. Include a description on the status and size of available prototype chambers.

This section should describe the technology up to the level of a single chamber.

B.1 Assembly

Describe the assembly procedure. Include details on

(a) Achieved mechanical precision of signal generating parts (i.e. strips or wires)

(b) Speed of assembly

(c) Splitting of work and logistics between production site

B.2 Quality Assurance and Commissioning

(a) Quality assurance of all individual chamber parts, include necessary manpower and rate of tests

(b) Quality assurance and commissioning scheme of full chambers, include necessary manpower and rate of tests

(c) How can/is data of the commissioning used later (e.g. strip or wire positions)?

Note: A common commissioning strategy during and after assembly of the wheels will be given in a previous chapter

B.3 Operation, Maintenance and Safety

Describe in detail the impact of failures of single components (gas leak, HV breakdown, front-end electronics) on the detector operation. Comment on possible built-in redundancy.

Describe in detail the possible scenarios for maintenance on the detector and the exchange or repair of detector parts.

Describe the risks associated with the technology during operation and maintenance (HV, maximum currents, flammable gas etc.)

B.4 Performance

Describe in detail the performance of the detector, including results from test beam studies. Include studies with background radiation (γ, n, p)

(a) Detector occupancy as function of rate

(b) Spatial and angular resolution as functions of rate and angle of incidence for single point measurements and segments

(c) Time resolution

(d) Efficiency (single measurement and segment)

(e) Double track resolution

(f) Rejection of fake and background tracks

(g) Sensitivity to background radiation

(h) Performance limits (maximum rate)

B.5 Aging Tests

Describe in detail results from aging tests for all components, the detector itself including the on-chamber gas distribution, read-out and/or trigger, alignment, and detector control electronics.

B.6 Cost, Funding, and Manpower

(a) Table of cost of each component, full chambers and total

(b) Additional costs (e.g. integrating two technologies)

(c) Arrangements for funding (if any so far)

(d) List of manpower needs, especially include statements on the the current and future availability of experts (for at least the full construction and commissioning period, i.e. 2012 – 2019, better also for the operation)

C TGC

D RPC

E Micromegas

References

[1] G. Aad et al. Expected Performance of the ATLAS Experiment - Detector, Trigger and Physics. 2009.

[2] G. Aad et al. The ATLAS Experiment at the CERN Large Hadron Collider. *JINST*, 3:S08003, 2008.